

## 2021-sCO<sub>2</sub>.eu-148

### UTILIZING INDUSTRIAL WASTE HEAT FOR POWER GENERATION USING sCO<sub>2</sub> CYCLE

**Soliman, Hady R.\***

KTH Royal Institute of Technology  
Energy Department  
Stockholm, Sweden  
hady@kth.se

**Börsson, Björn J.\***

KTH Royal Institute of Technology  
Energy Department  
Stockholm, Sweden  
bjto@kth.se

**Trevisan, Silvia**

KTH Royal Institute of Technology  
Energy Department  
Stockholm, Sweden

**Guédez, Rafael**

KTH Royal Institute of Technology  
Energy Department  
Stockholm, Sweden

#### ABSTRACT

The industrial sector accounts for approximately 30% of the global total energy consumption and 50% of that is lost as waste heat. Recovering waste heat from industries and utilizing it as an energy source is a sustainable way of generating electricity. Supercritical CO<sub>2</sub> (sCO<sub>2</sub>) cycles can be used with various heat sources including waste heat. Current literature primarily focuses on the cycle's thermodynamic performance without investigating the economics of the system. This is mainly due to the lack of reliable cost estimates for the cycle components. Recently developed cost scaling makes it possible to perform more accurate techno-economic studies on these systems. This work aims to model waste-heat-to-power systems and by performing sensitivity analysis on various system components, attempts to determine which factors require the most attention to bring this technology into commercialization. The industries with the largest unutilized waste heat are cement, iron and steel, aluminum and gas compressor stations. In this work, models of different sCO<sub>2</sub> cycle configurations were developed and simulated for these industries. The techno-economic model optimizes for the highest Net Present Value (NPV) using an Artificial Bee Colony algorithm. The optimization variables are the pressure levels, split ratios, recuperator effectiveness, condenser temperature and the turbine inlet temperature limited by the heat source. The results show industries can cut down costs by €8-34M using this system. Furthermore, the system can achieve an LCOE between 2.5-4.5 c€/kWh which is competitive with ORC (3.2-18 c€/kWh) and steam cycles (3-9 c€/kWh). Out of the modeled industries, waste heat recovery in the steel industry yields the highest NPV of €34.6M.

#### INTRODUCTION

The amount of CO<sub>2</sub> in the air has been increasing steadily with human activity. This has led to global warming, an increase of temperatures on the Earth. The power and industry sectors produce around 60% of global CO<sub>2</sub> emissions [1]. Several

solutions have been addressing this problem, by trying to reduce energy demand, reusing elements in a circular economy or using renewable energy. However, a solution that can allow industries to increase their energy efficiency which reduces electricity consumption from the power sector is utilizing their waste heat to produce electricity.

Hammond and Norman [2] calculated the waste heat coming out of industries in the UK, based on research and data gathered by McKenna and Norman [3]. Papapetrou et al. [4] continued that research by scaling it up for the EU, accounting for different energy intensities and energy efficiency improvements. They showed that for the EU alone, the potential of industrial waste heat is 314 TWh/year, with 33% at temperatures of 100-200°C (100 TWh/year), 25% between 200-500°C (78 TWh/year) and the rest above 500°C (124 TWh/year).

Campana et al. [5] analyzed 44 audits and feasibility studies of different factories. They found that the four industries with the highest potential for energy recovery within the EU were gas compression and storage facilities (10.5 TWh/year), the iron and steel industry (6.0 TWh/year), cement industry (4.6 TWh/year), and glass industry (0.6 TWh/year).

McKenna and Norman [3] concluded that even though the Aluminum industry has a lot of waste heat, most of it is low grade waste heat. Therefore, it is excluded from the analysis along with the glass industry.

The most common methods to generate power from waste heat are Kalina, Organic Rankine cycles (ORC), and conventional steam cycles. However, Kalina and ORCs are limited by their low efficiencies. The sCO<sub>2</sub> cycle is an emerging technology that can achieve high efficiencies over a broad range of temperatures and is able to utilize various heat sources. The system has compact components and is therefore significantly smaller than steam cycles, which can be very beneficial for waste heat recovery applications. Steam Rankine cycles require water conditioning and condensate control to avoid corrosion, fouling and scaling of components, whereas CO<sub>2</sub> is non-corrosive, non-

fouling and non-scaling. At medium temperatures,  $s\text{CO}_2$  is preferred over ORC due to its compactness, cost and high thermal efficiency [6]. These systems can be used for waste heat recovery from fuel cells [7], nuclear reactors [8], different industries and Concentrated Solar plants [9].

For the development of the  $s\text{CO}_2$  technology, modeling and simulation are essential to support decisions of investment and development. In this work a techno-economic model was developed to optimize the system performance in order to maximize the Net Present Value (NPV) of a waste heat recovery system. The optimization of thermal systems involves many decision variables and constraints. Conventional methods for this optimization apply an iterative procedure which may lead to solutions at local optimum. Advanced optimization algorithms, such as evolutionary and swarm intelligence-based algorithms, offer solutions to this problem. They are able to find a solution closer to the global optimum, with reasonable computational costs. Patel et al. [10] performed optimizations for various thermal systems using eleven of the most popular advanced optimization algorithms. They concluded that for the Brayton Power Cycle an algorithm called Artificial Bee Colony (ABC) was best suited for optimization of the system. The techno-economic model in this paper will therefore use that optimization algorithm for the  $s\text{CO}_2$  Brayton Cycle.

Several companies including Echogen, GE and Netpower along with various research facilities (Sandia, Oak Ridge, KAIST (Korea Advanced Institute of Science and Technology) have all been working on developing the  $s\text{CO}_2$  cycle. Within the EU, the EC has funded two projects (HeRo and Flex) [11]. They aim at developing a small-scale Brayton  $s\text{CO}_2$  cycle and a modular flexible coal power plant based on  $s\text{CO}_2$  cycle.

Recently General Electric, led by Vinnemier published a study on the usage of  $s\text{CO}_2$  cycles as storage in thermal power plants. Their modeling shows that the cycle can have a round trip efficiency of 60% [12].

Echogen has been working on a MW scale  $s\text{CO}_2$  cycle for waste heat recovery [13]. They have built a 2.4 MW plant to recover waste heat from a gas turbine using a simple recuperating cycle. Siemens Energy is also installing a  $s\text{CO}_2$  plant to recover the waste heat for Canadian energy company, TC Energy. It is expected to supply electricity for 10,000 homes this year [14].

## INDUSTRY DATA

Based on data from cement plants, the waste heat comes out at 300 °C with a flow rate of 74 kg/s from the preheaters and 40 kg/s from the clinker cooler as shown in Figure 1. The waste heat flow is relatively constant and has a specific heat capacity of 1.30 kJ/kg.K This was confirmed by an IFC report and Cembureau [15], [16]. In the iron and steel industry, a large source of waste heat is in the coke production process shown in Figure 2. By implementing a method called Coke Dry Quenching (CDQ) there are two high grade heat streams available for power production. First, is the inert gas used to cool down the coke which consists of 76.5%  $\text{N}_2$ , 12%  $\text{CO}_2$ , 8.5%  $\text{CO}$  and 3%  $\text{H}_2$ . Second, is the exhaust from the coke oven called Coke Oven Gas (COG) [17]. The EU produces 37 million tons of coke per year

in 62 facilities [18]. This is equivalent to coke production of 19 kg/s in an average facility resulting in 24 kg/s of waste gas flow, which varies little with time [17]. As for the COG, the average coke battery produces  $365 \text{ m}^3/\text{t}_{\text{coal}}$  of COG [19]–[21]. For an average size facility this is equivalent to a mass flow of 3.65 kg/s at constant rate [21].

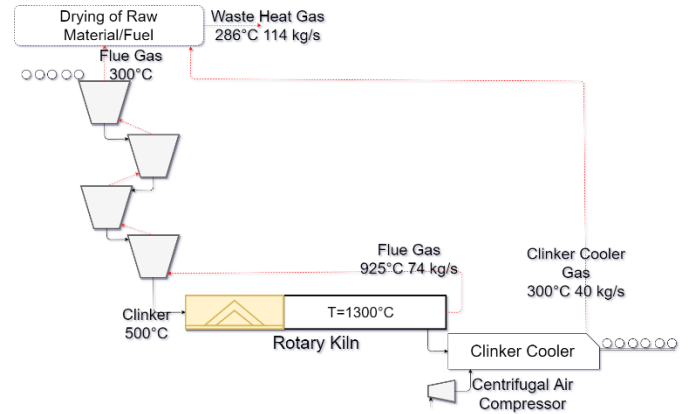


Figure 1: Material and energy streams in a cement plant.

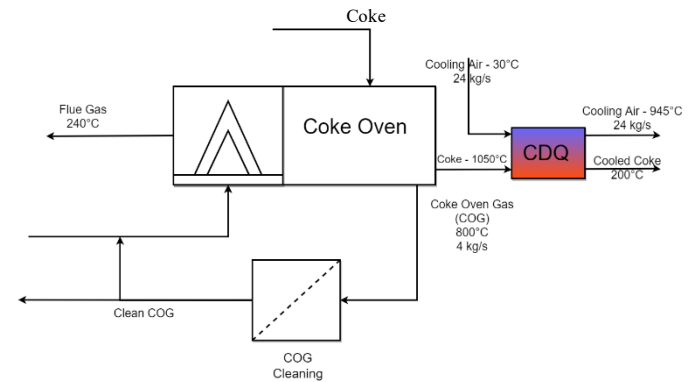


Figure 2: Material and energy streams in a coke plant.

Bianchi et al. [22] studied Gas Compression Stations (GCS) and investigated an average size compressor station and the amount of waste heat there. They concluded that the flue gas had a flow rate of 69 kg/s and temperature of 540°C. However, to account for backup units [5] and that gas compression do not run at constant load [23], a medium sized plant has a constant flow rate of 66 kg/s. The industrial waste heat fluid flow properties mentioned are summarized in Table 1 where:

$\dot{m}_{HS}$  is Waste Heat Mass Flow Rate (kg/s)

$T_{HS}$  is Waste Heat Temperature (°C)

$c_{p,HS}$  is Waste Heat Fluid Specific Heat Capacity (kJ/kg.K)

Table 1  
Industrial waste heat flows.

Industry	$T_{HS}$	$\dot{m}_{HS}$	$c_{p,HS}$
Cement Upstream	925	74	1.3
Cement Downstream	300	114	1.3
CDQ	945	24	$*a+bT+cT^2+dT^3$
GCS	520	66	1.68

\*coefficients (a,b,c,d) from [24].

## PERFORMANCE MODEL

The cycles that were modeled were the Simple Recuperated Brayton Cycle (SRBC) and the Recompression cycle which has been shown to have very high thermal efficiency [25]. Additional cycle configurations were investigated to compare their effectiveness for waste heat recovery applications. Hou et al. investigated two combined cycle configurations for waste heat recovery in gas turbines and the performance improvements

that they can offer for that application[26]. The Preheating and Dual Recuperated cycles were studied by Wright et al. for waste heat recovery applications and showed how they are better suited compared to the SRBC and Recompression cycle [27]. In this work all six of these cycle configurations are compared to further the understanding of which configuration is optimal for waste heat recovery applications. The cycles were modeled in MATLAB and are illustrated in Figure 3.

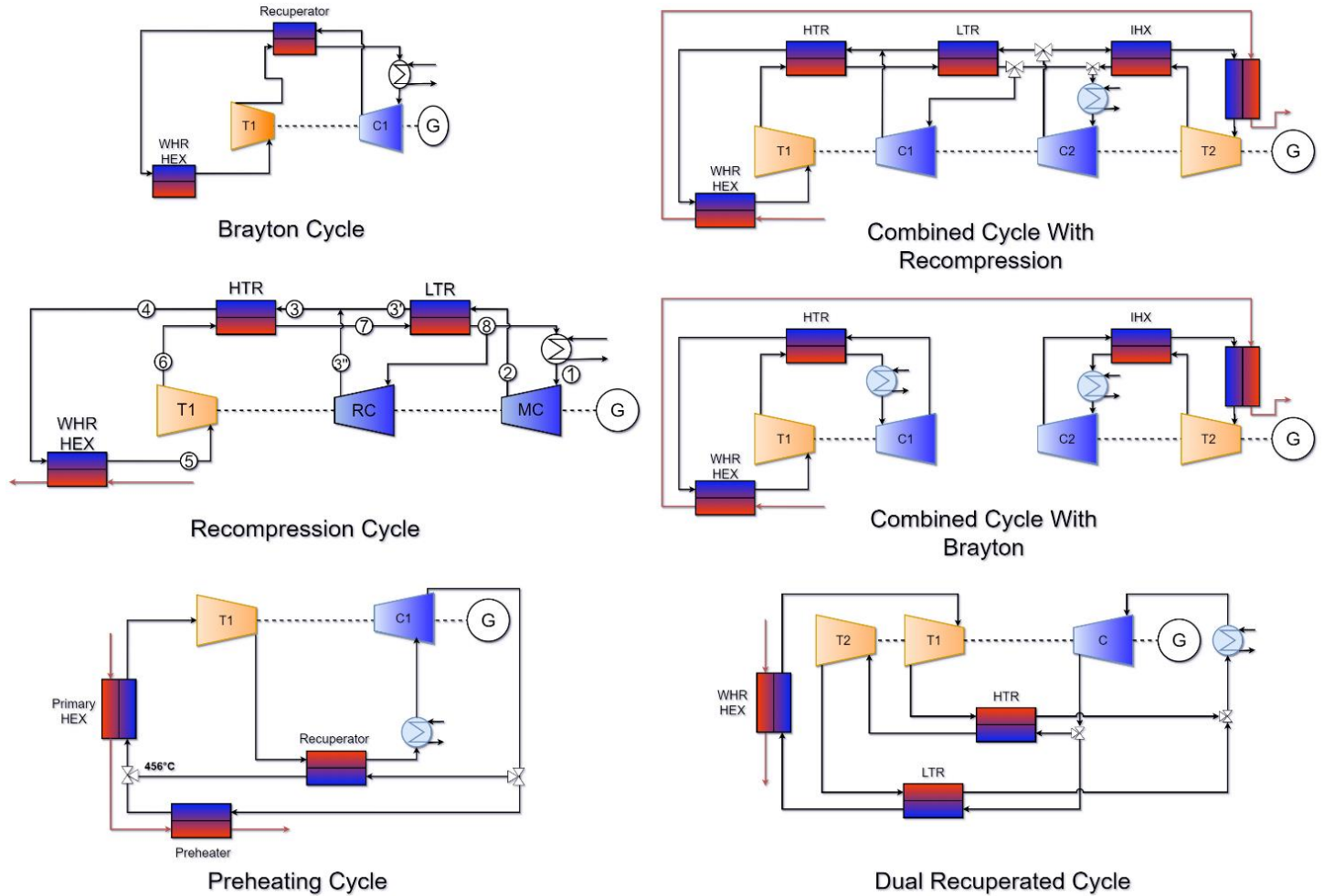


**Figure 3:** Supercritical CO<sub>2</sub> cycle configurations

The functionality of the model is demonstrated for the sCO<sub>2</sub> recompression cycle. Figure 4 demonstrates the logic flow of the techno-economic optimization model. It starts by reading inputs about the waste heat flow fluid properties mentioned in Table 1 along with the cooling medium temperature. Then, an initial population of employed bees is generated, i.e. a set of various design variables is generated. The design variables and their constraints are summarized in Table 2. The design variable for the temperature difference between the heat source  $T_{HS}$  and the Turbine Inlet Temperature (TIT) is dependent on which heat source is being utilized. Therefore, that design variable varies relative to the industry being investigated. A maximum value of 700°C for the turbine inlet temperature was used due to the

limitation of the turbine cost scaling model developed by Weiland et al. [28].

Table 2

Design variables for recompression cycle optimization.

Design Variable	Lower Bound	Upper Bound
High Pressure Level ( $P_h$ ), MPa	18.0	25.0
Low Pressure Level ( $P_l$ ), MPa	7.38	12.5
Split Ratio (SR)	0.5	1.0
Effectiveness of HTR ( $\epsilon_{HTR}$ )	0.550	0.999
Effectiveness of LTR ( $\epsilon_{LTR}$ )	0.550	0.999

Primary Heater Approach Temperature ( $\Delta T_{HS}$ ), °C	* $T_{HS} - 700$	$T_{HS} - 280$
Main Compressor inlet Temperature ( $T_1$ ), °C	32.0	50.0
Temperature Difference between Heat Source outlet and primary heat CO <sub>2</sub> inlet ( $\Delta T_{MH,out}$ ), °C	4	200

\*If  $T_{HS} < 704^\circ\text{C}$  then lower bound  $\Delta T_{HS} = 4$

### Turbomachinery

The design point performance of the turbine and compressors are modeled assuming adiabatic operation with a constant isentropic efficiency  $\eta_{is}$ . The fluid enters the turbomachinery with the specific enthalpy and entropy  $h_{in}$  and  $s_{in}$ . The isentropic specific enthalpy at the outlet  $h_{out,is}$  is then determined and the isentropic specific work  $w_{is}$  calculated using Equation 1

$$w_{is} = h_{in} - h_{out,is} \quad (1)$$

Using the definition of isentropic efficiency, the actual specific work ( $w$ ) for a turbine and a compressor can then be calculated using Equations (2) and (3) respectively.

$$w_{turbine} = w_{is} \cdot \eta_{is} \quad (2)$$

$$w_{compressor} = \frac{w_{is}}{\eta_{is}} \quad (3)$$

Finally, the specific enthalpy at the outlet can be calculated using Equation (4).

$$h_{out} = h_{in} - w \quad (4)$$

### Heat Exchangers (HEXs)

As can be seen in Figure 3, the recompression cycle consists of three different types of heat exchangers (two recuperators, primary heater and cooler). One of the challenges and interesting properties of sCO<sub>2</sub> is the change of its fluid properties around the critical point. Therefore, normal heat transfer correlations cannot be used for the modeling of an sCO<sub>2</sub> system [29].

### Recuperator

The recuperators are modeled assuming a counter-flow configuration. Three main working principles are utilized to calculate all four thermodynamic states at both sides of the recuperators. Firstly, the law of energy conservation across the HEX is used to calculate the final state when three are fully defined. Secondly, the definition of heat exchanger effectiveness, and lastly, the Log Mean Temperature Difference (LMTD) approach to determine the conductance of the HEX.

The fluid enters the hot and cold side of the recuperator with specific enthalpy ( $h_{h,in}, h_{c,in}$ ) and exits the hot side with

specific enthalpy ( $h_{h,out}$ ), all of which are determined from known temperatures and pressures.

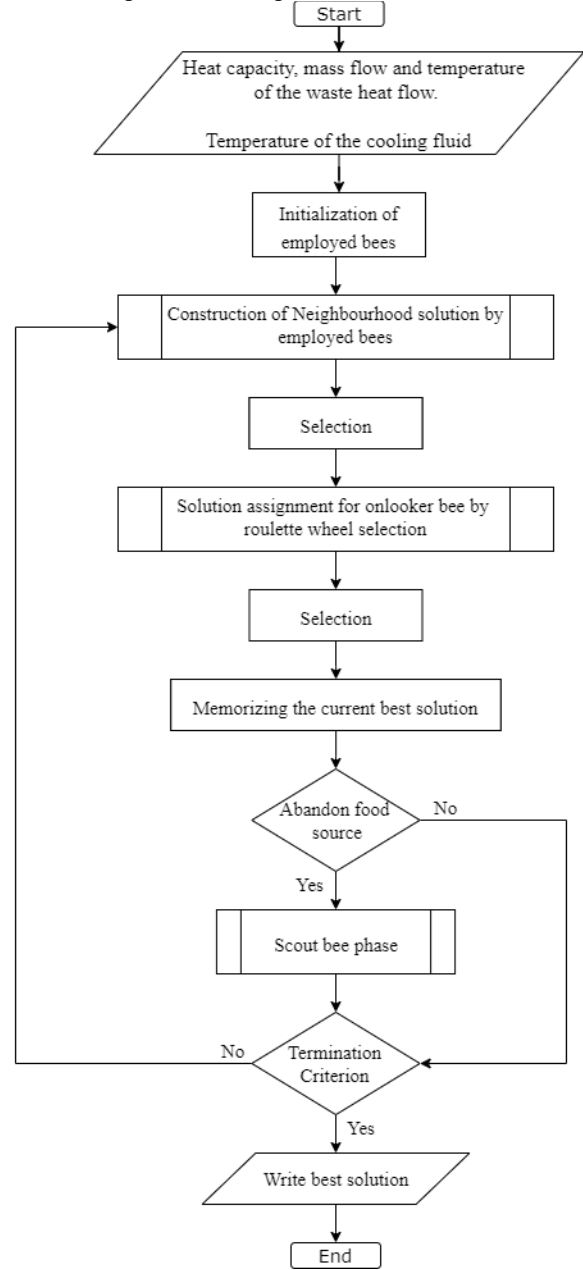


**FIGURE 4:** Optimization Model

Using the law of energy conservation, the cold side outlet specific enthalpy ( $h_{c,out}$ ) can be determined as shown by Equation (5):

$$h_{c,out} = h_{c,in} + \frac{\dot{m}_h \cdot (h_{h,in} - h_{h,out})}{\dot{m}_c} \quad (5)$$

For a recuperator that has the same fluid on both hot and cold sides this equation can be simplified. For the HTR the mass flow rate is equal on both sides and therefore cancel out. Due to the split flow in the recompression cycle the mass flow rates are

not equal but their ratio is known and is the split ratio (SR). Therefore Equation (5) is simplified to:

$$h_{c,out} = h_{c,in} + \frac{(h_{h,in} - h_{h,out})}{SR} \quad (6)$$

From the determined specific enthalpy and known pressure losses across the HEX all thermodynamic states are fully defined.

Equation (7) shows the definition of heat exchanger effectiveness.

$$\epsilon = \frac{\text{Actual heat transfer}}{\text{Maximum possible heat transfer}} = \frac{q}{q_{max}} \quad (7)$$

The actual heat transfer may be determined from either the energy lost by the hot fluid or the energy gained by the cold fluid, as shown in Equation (8).

$$q = \dot{m}_h c_h \cdot (T_{h,in} - T_{h,out}) = -\dot{m}_c c_c \cdot (T_{c,in} - T_{c,out}) \quad (8)$$

To calculate the maximum possible heat transfer, the maximum temperature difference present in the HEX is used, which is the difference between the inlet temperatures for the hot and cold fluids. Furthermore, the fluid that might undergo the maximum temperature difference is the one with the minimum value of  $\dot{m}c$ . The maximum possible heat transfer can then be determined using Equation (9).

$$q = (\dot{m}c)_{min} \cdot (T_{h,in} - T_{c,in}) \quad (9)$$

By selecting the appropriate side to calculate the actual heat transfer, the effectiveness can be determined by knowing the temperatures across the HEX. Equation (10) shows a general way of expressing the effectiveness.

$$\epsilon = \frac{\Delta T(\text{Minimum Fluid})}{\text{Maximum Temperature Difference in heat Exchanger}} \quad (10)$$

The minimum fluid is always the one undergoing the larger temperature change in the heat exchanger. The maximum temperature difference in the heat exchanger is always the temperature difference of the hot and cold fluid inlets [30].

The heat transfer rate across a heat exchanger can be expressed using the LMTD method according to Equation (11).

$$\dot{Q} = (UA)\Delta T_{LMTD} \quad (11)$$

where  $\Delta T_{LMTD}$  for a counter-flow configuration can be expressed as,

$$\Delta T_{LMTD} = \frac{(T_{h,out} - T_{c,in}) - (T_{h,in} - T_{c,out})}{\ln\left(\frac{T_{h,out} - T_{c,in}}{T_{h,in} - T_{c,out}}\right)} \quad (12)$$

This method involves two important assumptions. First one is that the specific heats of the fluids do not vary with temperature,

and the second that the convection heat transfer coefficients are constant throughout the heat exchanger. In the case of sCO<sub>2</sub> cycles, both these assumptions are likely to be broken due to the large variations in thermodynamic properties of CO<sub>2</sub> under supercritical conditions. Therefore, to accurately capture the effects of changing fluid properties, each heat exchanger is discretized into sub-section connected in series [31].

Using this approach, the total conductance of a recuperator is determined using the known inlet and outlet conditions. The total heat transfer rate ( $\dot{Q}$ ) through the heat exchanger is calculated and evenly distributed amongst the discretized sub-sections. Assuming that the pressure losses across the HEX are linear, the inlet and outlet states for each sub-section can be fully defined. Using Equation (11) the conductance of each sub-section can be determined:

$$(UA)_i = \frac{\dot{Q}_i}{\Delta T_{LMTD,i}} \quad (12)$$

The total conductance for the recuperator is then the sum of all sub-section conductance values.

$$(UA) = \sum (UA)_i \quad (13)$$

## B. Primary Heater

From the approach described above the thermodynamic properties at every point in the sCO<sub>2</sub> cycle can be determined. From the known fluid properties of the waste heat, the total heat transfer rate of the heat exchanger can be calculated. An energy balance across the heat exchanger can then be used to calculate the mass flow rate of CO<sub>2</sub>. Following the same approach of the recuperators, the total conductance of the primary heat exchanger can be calculated.

## C. Cooler:

An air-cooling system for Brayton cycles conventionally has cross-flow configuration. Since a cross-flow heat exchanger has two fluid flows in perpendicular directions, a fluid flowing in parallel channels will observe opposite side fluids at different temperatures. This means that numerical modeling of this system needs to be two-dimensional, resulting in huge increase in computation cost [32]. Therefore, to improve computation time, a simplification is made by assuming an approach temperature of 15°C and calculating the heat exchanger conductance using the known temperatures on the CO<sub>2</sub> side.

The subroutine of solution assignments for the various bee groups, mentioned in Figure 4, represents the evaluation of a food source that an individual bee has found. The subroutine uses generated design variables for a food source and calculates the solution, or fitness, at that particular location. A flow diagram of the model iteration logic for that subroutine can be seen in Figure 5. The approach follows a similar approach as Dyreby [33] aside from the different design variable inputs. These alterations were made for optimizing waste heat recovery applications specifically.

The operating assumptions for the sCO<sub>2</sub> waste heat recovery cycles are shown in Table 3 [34]. The open source C++ library named CoolProp was used to obtain fluid properties [35].

Table 3  
Operating assumptions for the sCO<sub>2</sub> cycle.

sCO <sub>2</sub> Assumption	Symbol	Value
Compressor isentropic efficiency	$\eta_{comp}$	89%
Turbine isentropic efficiency	$\eta_{turbine}$	93%
Generator efficiency	$\eta_{gen}$	98%
Cooling fluid inlet temperature	TCS	25 °C

During this iterative process it is possible for a temperature cross-over to occur, a condition where the hot side temperature drops below the cold side temperature in a particular region on a particular iteration. In this instance the method of calculating the UA value would give a complex number. This occurrence implies that the results for this iteration are non-physical due to a violation of the Second Law of Thermodynamics. This situation is handled by checking whether all conductance values are real numbers. If not, the fitness function returns a value of negative infinity so that the optimization algorithm ignores that solution. A limitation of the optimization algorithm is the fact that there will always be a possibility of not finding the global optimum. However, the success rate of the ABC algorithm for Brayton power cycle optimization has been found to be 96% [10]. Therefore, by running each calculation 10 times and using the best value, means that the approach should only fail to find the global optimum once every 100 Trillion times.

Like the model developed by Dyreby [33], a combination of the secant and bisection methods are used for both iteration loops to adjust  $T_7$  and  $T_8$ . Even though the secant method has a higher rate of convergence, it can potentially predict new values outside of valid bounds, leading to divergence of the method. By reverting back to the bisection method when the secant method fails this can be avoided [36].

## ECONOMIC MODEL

The economic assumptions used to calculate the cycle's KPIs for the optimization algorithm are shown in Table 4.

Table 4  
Economic Assumptions Used in Calculating KPIs

Economic Assumptions	Symbol	Value
Nominal Discount Rate	$i$	6%
Lifetime	$n$	25 years
Annual Operating Hours	$N_h$	7446 hours (15%)
Electricity Price	$el_{price}$	€0.065/kwh <sub>e</sub>

The NPV was calculated using equation (14), where  $E_t$  is the electricity generated. The assumed electricity price was based on the prices that the surveyed European cement plants pay.

$$NPV = \sum_{t=0}^n \frac{el_{price} \times E_t - costs}{(1+i)^n} \quad (14)$$

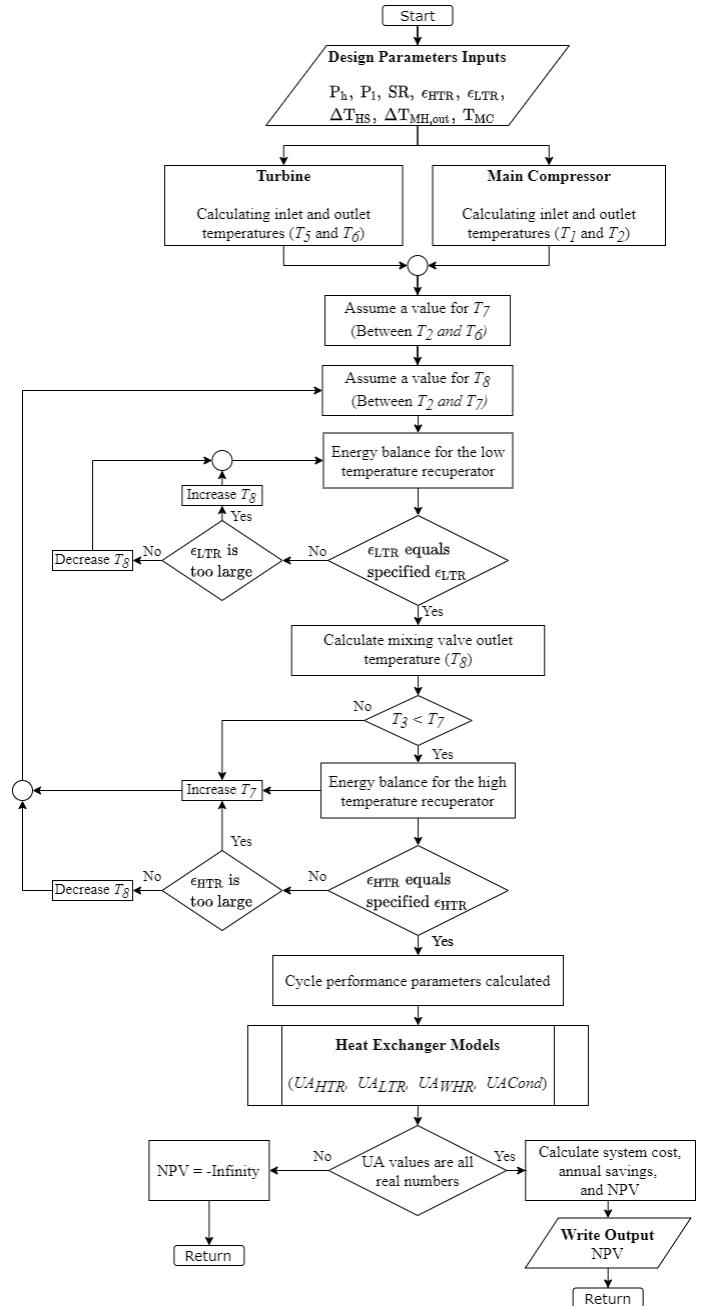


Figure 5: Iterative process logic flow for the cycle model

Thermal efficiency is defined as the ratio between electrical power produced by the cycle ( $\dot{P}_e$ ) and thermal power extracted from the heat source ( $\dot{Q}_{th}$ ).

$$n_{th} = \frac{\dot{P}_e}{\dot{Q}_{th}} \quad (15)$$

Exergy Efficiency is defined as the ratio between electrical power produced by the sCO<sub>2</sub> power cycle and available heat in the waste heat exhaust ( $Q_{exhaust}$ ).

$$n_{ex} = \frac{\dot{P}_e}{\dot{Q}_{exhaust}} \quad (16)$$

Waste Heat utilization is defined as the ratio of waste heat transferred to the sCO<sub>2</sub> cycle ( $Q_{WHEX}$ ) relative to the available heat in the waste heat exhaust.

$$WHU = \frac{Q_{WHEX}}{Q_{exhaust}} \quad (17)$$

Levelized Cost of electricity is defined as the net present cost of electricity generation for a generating plant over its lifetime [37].

$$LCOE = \frac{\text{sum of costs over time}}{\text{sum of power generated}} = \frac{\sum_{t=0}^n \frac{\text{Costs}}{(1+i)^t}}{\sum_{t=0}^n \frac{E_t}{(1+i)^t}} \quad (18)$$

Weiland et al. [28] recently developed a cost scaling model for the components in a sCO<sub>2</sub> cycle. The model is based on a total of 129 vendor quotes, and spans cycle size ranges of 5-750 MW<sub>e</sub>. It uses an appropriate scaling parameter (SP) for different components and includes a temperature correction factor  $f_T$  for certain components to account for the increase in cost at higher temperatures. The cost scaling can be expressed in a general way using Equation (18).

$$C_E = a \cdot SP^b \cdot f_T \quad (18)$$

where,

$$f_T = \begin{cases} 1, & \text{if } T_{max} < T_{bp} \\ (1 + c \cdot (T_{max} - T_{bp}) + d \cdot (T_{max} - T_{bp})^2), & \text{if } T_{max} \geq T_{bp} \end{cases}$$

and  $C_E$  is the equipment cost for an individual cycle component,  $a$  is the reference cost, and  $b$  is the cost exponent in order to consider economy of scale. Reference costs and exponents are from Weiland et al. [28].

The direct equipment capital cost ( $C_{DE}$ ) is calculated according to Bailie et al. [38], and can be expressed on a general form as Equation (19):

$$C_{DE} = C_E \cdot (1 + \alpha_M)(1 + \alpha_L) \quad (19)$$

where  $\alpha_m$  and  $\alpha_L$  are the multiplication factors for installation cost of materials and labor, respectively. These factors are also based on Weiland et al. [28]. System piping costs can vary anywhere between 5-20% of total power block capital costs, depending on the cycle operating conditions [39]. For the analysis performed in this research a value of 10% was used. Additionally, direct capital accounting for improvements to site, instrumentation and controls, and other miscellaneous Balance of Plant (BOP) systems are also added [40].

Indirect costs include Engineering, Procurement and Construction cost (EPC) along with contingencies. The EPC costs are assumed to be 9% of the total direct capital cost [41]. The contingencies depend on the status of the technology being considered and are assumed to be 30% of the combined direct capital expenditures and EPC cost [42].

Operation and Maintenance (O&M) costs include taxes, maintenance material costs, and labor costs that account for operating, maintenance, administrative and support labor [43]. A correction factor of 25% was included to exclude the costs associated with the coal gasification section of the power plant modeled by Weiland et al. [43].

## RESULTS

Different industries were analyzed in this model. The inputs into the model are mentioned in Performance Model section. Table 5 shows the optimal cycle configuration and net power output for each industry. Figure 6 shows the NPV, LCOE and the Payback Period (PP) of the industries. Figure 7 shows the CO<sub>2</sub> mitigated and efficiencies per industry.

Table 5  
Optimum cycle configuration and size for each industry.

Industry	Configuration	Net Power Output [MW]
Cement Upstream	SRBC	9.4
Cement Downstream	SRBC	5.5
CDQ	Preheating	10.9
GCS	Preheating	13

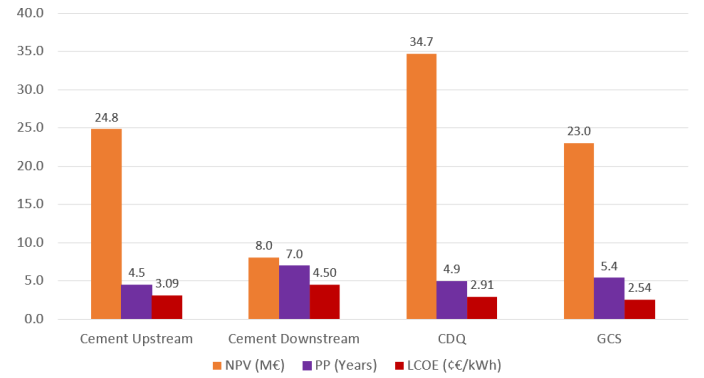


Figure 6: NPV and PP of the waste heat recovery systems.

The sCO<sub>2</sub> cycle for these industries yielded LCOEs between 2.5-4.5 c€/kWh. Waste heat recovery applications using ORC systems can achieve LCOE between 3.2-18 c€/kWh [44]–[47]. Previous studies on waste heat recovery using steam cycles have found them to achieve an LCOE between 3-9 c€/kWh [37,39]. While these ranges are relatively similar, sCO<sub>2</sub> cycles have the additional benefits of compactness and less water consumption.

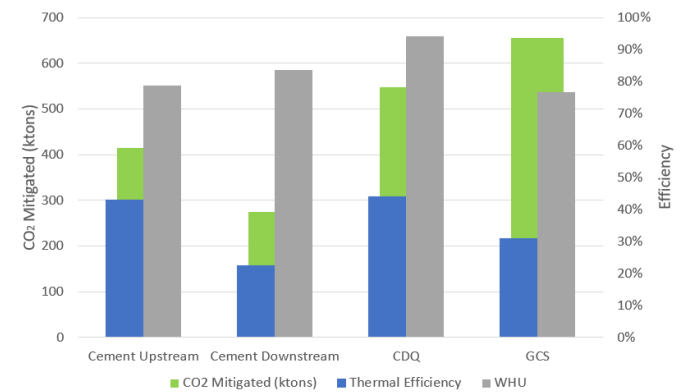
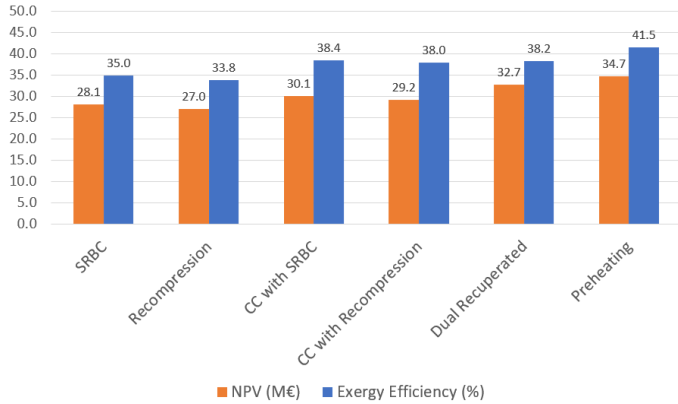


Figure 7: Mitigated emissions, thermal efficiency and waste heat utilization of the waste heat recovery systems.

A modern cement facility utilizes 60% of the available waste heat using 4-stage preheater. The addition of a downstream or

upstream sCO<sub>2</sub> cycle would result in 84% or 79% waste heat utilization, respectively. Therefore, as can be seen in Figure 7, the downstream and upstream sCO<sub>2</sub> cycles utilize additional 24% and 19% waste heat, respectively.

To compare between different cycle configurations, the CDQ process in the Iron and Steel industry is used. The different cycle efficiencies and NPVs are shown in Figure 8. The preheating cycle yields the highest exergy efficiency and NPV.



**Figure 8:** NPV and exergy efficiency of the different cycle configurations for Coke Dry Quenching.

*Effect of Split Ratio on NPV*

Recompression cycle has been gaining a lot of attention in the past years due to its high thermal efficiency. Figure 8 shows that the other cycle configurations all yield a higher NPV than the Recompression cycle. As can be seen in Figure 9, the thermal efficiency increases as the split ratio decreases until it reaches a maximum. On the other hand, the NPV decreases as the split ratio decreases. This means that it is more economic to use a SRBC than a recompression cycle. Even though recompression cycles can give higher thermal efficiencies, they are limited by their ability to utilize waste heat sources resulting in lower NPV and exergy efficiency. The NPV has a sharp increase around split ratio of 0.65 which is due to the system being able to use a smaller and less expensive motor to drive the recompressor.

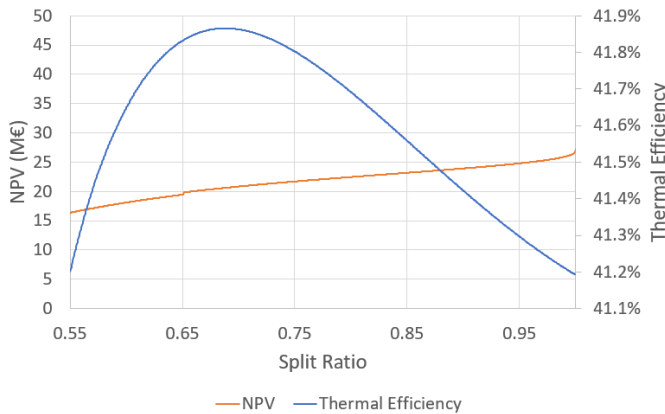


**Figure 9:** NPV and thermal efficiency at different split ratio for the Recompression Cycle.

*System Costs*

The power block has the highest contribution to the Capital Expenditures (CAPEX) as can be seen in Figure 10. The CDQ WHR (Waste Heat Recovery) section also has a large share of the total cost, or 31%. This is because it has an intermediate loop using inert gas as heat transfer fluid. Since this is a relatively new technology, the contingencies cost is also high at 16% of the CAPEX cost.

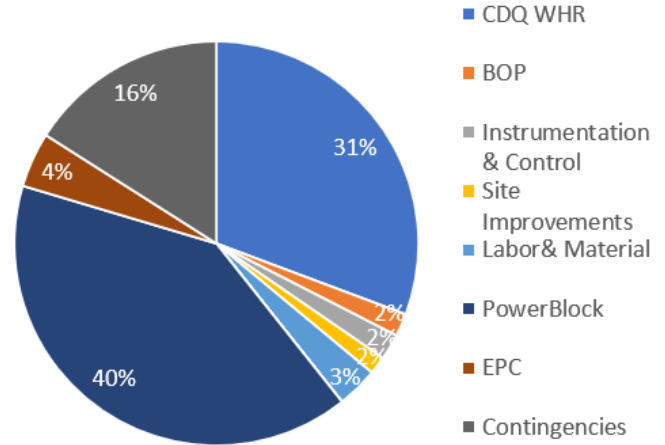


**Figure 10:** CAPEX share among main plant components

*Sensitivity Analysis*

A sensitivity analysis is carried out to determine which factors affect the NPV mostly. The error ranges of the cost model [28] are chosen as the sensitivity ranges. Results show that the components' price do not affect the NPV significantly. Were the power block to increase in cost by 35% the NPV increases by only 13%. This shows that the uncertainty in the cost estimation model will not greatly impact the NPV. Among the different components, the compressor's cost has the greatest impact. Figure 11 shows the impact of the change in price of all power block components.

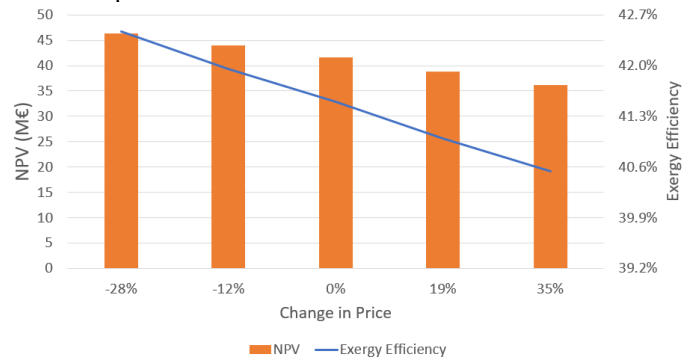


**Figure 11:** Sensitivity Analysis of Change in Power Block Price

For the other factors, the electricity price has the highest impact on NPV as can be seen in Figure 12. An increase in the electricity price of 29% would increase the NPV by 37%.



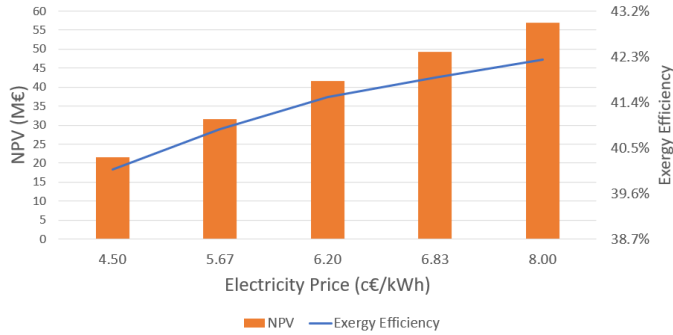


**Figure 12:** Sensitivity Analysis of Change in Electricity Price

## CONCLUSION

In this work the relationship between thermal efficiency, exergy efficiency, and cost of the sCO<sub>2</sub> power cycles for waste heat recovery was investigated.

The optimal trade-off between the economics and thermodynamic performance of an sCO<sub>2</sub> cycle was estimated using a techno-economic optimization structure of the different cycle parameters. The approach compares six different cycle configurations and optimizes for the highest NPV cycle. The pressure levels of the cycle along with the recuperators' effectiveness were optimized for the different industries and configurations to yield the highest NPV.

The results show that sCO<sub>2</sub> cycles can be competitive on an LCOE basis with both ORC and steam cycles for waste heat recovery applications.

With the constraints assumed in this work, the highest NPV for a medium size coke dry quenching process in an iron and steel plant was €34.6M. This system had a thermal efficiency of 44%, a payback period of 4.9 years and LCOE of 2.91 c€/kWh. It was deduced that even with their higher thermal efficiencies, recompression cycles provide lower economic value for waste heat recovery. This is due to their limited temperature glide in the primary heater, resulting in lower waste heat utilization. It was discovered that the preheating cycle is best suited among the cycles analyzed.

The turbomachinery needed to operate this cycle is a concern. CO<sub>2</sub> has high density at supercritical conditions, which makes the machinery required compact. However, this also means higher stresses on the blades, this might prohibit the use of single shaft machines with few stages. Assessing these thermomechanical stresses may be an important factor to include while modeling these systems, which was excluded in the cost models that were used in this work.

More analysis is needed for (a) the cycle operation with variable waste heat (b) operation at off-design point, (c) the investigation of start-ups, shut-downs and load changes and (d) dual operation of compressors as turbines and vice versa. Future work will focus on supercritical cycle systems at large scale to properly evaluate their commercialization.

## NOMENCLATURE

ABC Artificial Bee Colony  
BOP Balance of Plant

CAPEX Capital Expenditures  
CC Combined Cycle  
CDQ coke dry quenching  
COG Coke Oven Gas  
 $c_p$  Specific Heat Capacity  
 $c_{p,HS}$  Waste Heat Fluid Specific Heat Capacity  
 $\epsilon$  Effectiveness  
 $E_{l,price}$  electricity price  
EPC Engineering, Procurement and Construction  
GCS Gas Compression Station  
 $h$  Enthalpy  
HEX Heat Exchanger  
HTR High Temperature Recuperator  
 $i$  Nominal Discount Rate  
LCOE Levelized Cost Of Energy  
LMTD Log Mean Temperature Difference  
LTR Low Temperature Recuperator  
 $\dot{m}_{HS}$  Waste Heat Mass Flow Rate  
 $n$  Efficiency  
 $n$  Lifetime  
 $N_h$  Annual Operating Hours  
NPV Net Present Value  
O&M Operation and Maintenance  
ORC Organic Rankine Cycle  
PP Payback Period  
SR Split Ratio  
SRBC Simple Recuperated Brayton Cycle  
sCO<sub>2</sub> Supercritical Carbon Dioxide  
 $T_{HS}$  is Waste Heat Temperature  
TIT Turbine Inlet Temperature  
UA Heat Exchanger Conductance  
WHU Waste Heat Utilization  
WHR Waste Heat Recovery  
 $w_{is}$  Isentropic Specific Work

## ACKNOWLEDGEMENTS

We would like to thank Francesco Campana for the work he carried out in estimating the waste heat potential in EU. We would also like to thank him for explaining to us the methodology they used. Special thanks to the managers of the cement plants that answered our questions. We are grateful for Rafael Guédez and Silvia Trevisan who gave us a lot of resources and guided our way of thinking.

## REFERENCES

- [1] Lead, "Sources of CO<sub>2</sub>," CARBON DIOXIDE CAPTURE AND STORAGE, p. 75.
- [2] G. P. Hammond and J. B. Norman, (2014), "Heat recovery opportunities in UK industry," Appl. Energy, vol. 116, pp. 387–397.
- [3] R. C. McKenna and J. B. Norman, (2010), "Spatial modelling of industrial heat loads and recovery potentials in the UK," Energy Policy, vol. 38, no. 10, pp. 5878–5891.
- [4] M. Papapetrou, G. Kosmadakis, A. Cipollina, U. La Commare, and G. Micale, (2018), "Industrial waste heat: Estimation of the technically available resource in the EU per industrial sector, temperature level and country,"

- Appl. Therm. Eng., doi: 10.1016/j.applthermaleng.2018.04.043.
- [5] F. Campana *et al.*, (2013), “ORC waste heat recovery in European energy intensive industries: Energy and GHG savings,” *Energy Convers. Manag.*, vol. 76, pp. 244–252.
- [6] X. Wang and Y. Dai, (2016), “Exergoeconomic analysis of utilizing the transcritical CO<sub>2</sub> cycle and the ORC for a recompression supercritical CO<sub>2</sub> cycle waste heat recovery: A comparative study,” *Appl. Energy*, vol. 170, pp. 193–207.
- [7] D. Sanchez, J. M. M. de Escalona, R. Chacartegui, A. Munoz, and T. Sanchez, (2011), “A comparison between molten carbonate fuel cells based hybrid systems using air and supercritical carbon dioxide Brayton cycles with state of the art technology,” *J. Power Sources*, vol. 196, no. 9, pp. 4347–4354.
- [8] L. Dunhuang, Z. Yaoli, and G. U. O. Qixun, (2015), “Modeling and analysis of nuclear reactor system using supercritical-CO<sub>2</sub> brayton cycle,” *J. Xiamen Univ. (Natural Sci.)*, vol. 54, no. 5, pp. 608–613.
- [9] R. Singh, S. A. Miller, A. S. Rowlands, and P. A. Jacobs, (2013), “Dynamic characteristics of a direct-heated supercritical carbon-dioxide Brayton cycle in a solar thermal power plant,” *Energy*, vol. 50, pp. 194–204.
- [10] V. K. Patel, V. J. Savsani, and M. A. Tawhid, *Thermal System Optimization - A Population-Based Metaheuristic Approach* *{\vert\$}* Vivek K. Patel *{\vert\$}* Springer. Springer International Publishing, 2019.
- [11] “sCO<sub>2</sub>-flex.” 2019.
- [12] P. Vinnemeier, M. Wirsum, D. Malpiece, and R. Bove, (2016), “Integration of heat pumps into thermal plants for creation of large-scale electricity storage capacities,” *Appl. Energy*, vol. 184, pp. 506–522.
- [13] T. J. Held, “Initial test results of a megawatt-class supercritical CO<sub>2</sub> heat engine,” in *The 4th International Symposium–Supercritical CO<sub>2</sub> Power Cycles*, 2014 2014, pp. 9–10.
- [14] F. Krull, “Power from waste heat: Maximum yield with supercritical carbon dioxide,” *Siemens Energy*. [Online]. Available: <https://www.siemens-energy.com/global/en/news/magazine/2020/waste-heat-to-power-with-sco2-turbines.html>.
- [15] A. Doğan *et al.*, “Waste heat recovery in Turkish cement industry: review of existing installations and assessment of remaining potential,” (2018).
- [16] Cembureau, “Key Facts & Figures.” 2019.
- [17] S. Qin and S. Chang, (2017), “Modeling, thermodynamic and techno-economic analysis of coke production process with waste heat recovery,” *Energy*, vol. 141, pp. 435–450.
- [18] Eurostat, “Eurostat - Data Explorer.” Aug. 2020.
- [19] S. Ndlovu, G. S. Simate, and E. Matinde, *Waste production and utilization in the metal extraction industry*. CRC Press, 2017.
- [20] K. C. Tran, G. Harp, O. Sigurbjörnsson, C. Bergins, and T. Buddenberg, (2016), “Carbon Recycling for Converting Coke Oven Gas to Methanol for the Reduction of Carbon Dioxide at Steel Mills,” *MefCO<sub>2</sub>: Auderghem*, Belgium.
- [21] Satyendra, “Coke Oven Gas, its Characteristics and Safety Requirements – IspatGuru.” 2015.
- [22] M. Bianchi *et al.*, (2017), “Techno-economic analysis of ORC in gas compression stations taking into account actual operating conditions,” *Energy Procedia*, vol. 129, pp. 543–550.
- [23] S. L. Gómez-Alález, V. Brizzi, D. Alfani, P. Silva, A. Gostri, and M. Astolfi, (2017), “Off-design study of a waste heat recovery ORC module in gas pipelines recompression station,” *Energy Procedia*, vol. 129, pp. 567–574.
- [24] T. M. Miller, “CRC Handbook of Chemistry and Physics 88th edn, ed DR Lide.” Boca Raton, FL: CRC Press, 2008.
- [25] K. Wang, M.-J. Li, J.-Q. Guo, P. Li, and Z.-B. Liu, (2018), “A systematic comparison of different S-CO<sub>2</sub> Brayton cycle layouts based on multi-objective optimization for applications in solar power tower plants,” *Appl. Energy*, vol. 212, pp. 109–121.
- [26] S. Hou, Y. Wu, Y. Zhou, and L. Yu, (2017), “Performance analysis of the combined supercritical CO<sub>2</sub> recompression and regenerative cycle used in waste heat recovery of marine gas turbine,” *Energy Convers. Manag.*, vol. 151, pp. 73–85.
- [27] S. A. Wright, C. S. Davidson, and W. O. Scammell, “Thermo-economic analysis of four sCO<sub>2</sub> waste heat recovery power systems,” in *Fifth International SCO<sub>2</sub> Symposium, San Antonio, TX, Mar, 2016* 2016, pp. 28–31.
- [28] N. Weiland, B. Lance, and S. Pidaparti, “sCO<sub>2</sub> Power Cycle Component Cost Correlations from DOE Data Spanning Multiple Scales and Applications (Final),” (2019).
- [29] L. F. Cabeza, A. de Gracia, A. I. Fernández, and M. M. Farid, (2017), “Supercritical CO<sub>2</sub> as heat transfer fluid: A review,” *Appl. Therm. Eng.*, vol. 125, pp. 799–810.
- [30] J. Holman, *Heat Transfer (Int’l Ed)*. McGraw-Hill Education / Asia, 2018.
- [31] G. Nellis and S. Klein, *Heat Transfer*. Cambridge University Press, 2012.
- [32] A. Moisseytsev, J. J. Sienicki, and Q. Lv, “Dry Air Cooler Modeling for Supercritical Carbon Dioxide Brayton Cycle Analysis,” doi: 10.2172/1342159.
- [33] J. J. Dyreby, “Modeling the supercritical carbon dioxide Brayton cycle with recompression,” *The University of Wisconsin-Madison*, 2014.
- [34] S. Trevisan, R. Guédez, and B. Laumert, “Supercritical CO<sub>2</sub> Brayton Power Cycle for CSP With Packed Bed TES Integration and Cost Benchmark Evaluation,” in *ASME Power Conference*, 2019 2019, vol. 59100, p. V001T06A010.

- [35] I. H. Bell, J. Wronski, S. Quoilin, and V. Lemort, (2014), "Pure and Pseudo-pure Fluid Thermophysical Property Evaluation and the Open-Source Thermophysical Property Library CoolProp," *Ind. Eng. Chem. Res.*, vol. 53, no. 6, pp. 2498–2508, doi: 10.1021/ie4033999.
- [36] R. Canale and S. Chapra, *Numerical Methods for Engineers*. McGraw-Hill Science/Engineering/Math, 2009.
- [37] I. IRENA, (2019), "Renewable power generation costs in 2018. Report," *Int. Renew. Energy Agency*, Abu Dhabi.
- [38] R. C. Bailie, W. B. Whiting, J. A. Shaeiwitz, R. Turton, and D. Bhattacharyya, *Analysis, Synthesis, and Design of Chemical Processes*. Pearson, 2018.
- [39] C. White, D. Gray, J. Plunkett, W. Shelton, N. Weiland, and T. Shultz, "Techno-economic Evaluation of Utility-Scale Power Plants Based on the Indirect sCO<sub>2</sub> Brayton Cycle." Sep. 2017.
- [40] C. W. White, W. W. Shelton, N. T. Weiland, and T. R. Shultz, "sCO<sub>2</sub> Cycle as an Efficiency Improvement Opportunity for Air-fired Coal Combustion," in *The 6th International Supercritical CO<sub>2</sub> Power Cycles Symposium*, 2018 2018, pp. 27–29.
- [41] M. Turner and A. T. Samaei, "Quality Guidelines for Energy System Studies: Capital Cost Scaling Methodology: Revision 3 Reports and Prior," (2019).
- [42] K. Gerdes, W. M. Summers, and J. Wimer, "Quality Guidelines for Energy System Studies: Cost Estimation Methodology for NETL Assessments of Power Plant Performance," (2011).
- [43] N. Weiland, W. Shelton, T. Shultz, C. W. White, and D. Gray, "Performance and Cost Assessment of a Coal Gasification Power Plant Integrated with a Direct-Fired sCO<sub>2</sub> Brayton Cycle," (2017).
- [44] C. E. C. Rodríguez *et al.*, (2013), "Exergetic and economic comparison of ORC and Kalina cycle for low temperature enhanced geothermal system in Brazil," *Appl. Therm. Eng.*, vol. 52, no. 1, pp. 109–119.
- [45] R. Pili, A. Romagnoli, H. Spliethoff, and C. Wieland, (2017), "Techno-economic analysis of waste heat recovery with ORC from fluctuating industrial sources," *Energy procedia*, vol. 129, pp. 503–510.
- [46] C. Zhang, A. Romagnoli, J. Y. Kim, A. A. M. Azli, S. Rajoo, and A. Lindsay, (2017), "Implementation of industrial waste heat to power in Southeast Asia: an outlook from the perspective of market potentials, opportunities and success catalysts," *Energy Policy*, vol. 106, pp. 525–535.
- [47] A. Doğan *et al.*, "Waste heat recovery in Turkish cement industry: review of existing installations and assessment of remaining potential," *The World Bank*, (2018).
- [48] M. Persichilli, T. Held, S. Hostler, E. Zdankiewicz, and D. Klapp, (2011), "Transforming waste heat to power through development of a CO<sub>2</sub>-based-power cycle," *Electr. Power Expo*, vol. 10.

# DuEPublico

Duisburg-Essen Publications online

UNIVERSITÄT  
DUISBURG  
ESSEN

*Offen im Denken*

ub | universitäts  
bibliothek

*Published in: 4th European sCO<sub>2</sub> Conference for Energy Systems, 2021*

This text is made available via DuEPublico, the institutional repository of the University of Duisburg-Essen. This version may eventually differ from another version distributed by a commercial publisher.

**DOI:** 10.17185/duepublico/73976

**URN:** urn:nbn:de:hbz:464-20210330-121134-5



This work may be used under a Creative Commons Attribution 4.0 License (CC BY 4.0).